Comparison of some analytically and numerically calculated parameters for toroidal field coils

M. Söll

IPP 4/145 November 1976

MAX-PLANCK-INSTITUT FÜR PLASMAPHYSIK

8046 GARCHING BEI MÜNCHEN

MAX-PLANCK-INSTITUT FÜR PLASMAPHYSIK

GARCHING BEI MÜNCHEN

Comparison of some analytically and numerically calculated parameters for toroidal field coils

M. Söll

IPP 4/145 November 1976

Die nachstehende Arbeit wurde im Rahmen des Vertrages zwischen dem Max-Planck-Institut für Plasmaphysik und der Europäischen Atomgemeinschaft über die Zusammenarbeit auf dem Gebiete der Plasmaphysik durchgeführt.

IPP 4/145

Comparison of some analytically and numerically calculated parameters for toroidal field coils

M. Söll

November 1976

Abstract

In this paper, a comparison is made between toroidal coil parameters calculated analytically and numerically by computer programs. One reason for this comparison is that in the case of good agreement between numerically and analytically calculated parameters one can save computing time especially for parameter studies.

As parameters investigated in this work we have chosen the maximum magnetic field, the radial magnetic force per unit length exerted on the conductor and the centering force per coil. The investigations were carried out for circular and D-coils.

We also compare the stresses in a superconducting circular coil for which the magnetic volume forces are calculated analytically and numerically.

TABLE OF CONTENTS

1. THEORETICAL BASIS

1.1 Ideal toroidal field coil system

The ideal toroidal field magnet system consists of a thin one--layer shell of uniformly wound conductors. In this case, the finite number of coils and the size of the winding cross-section are disregarded. The toroidal magnetic field for the ideal case inside the coil is given by

$$B(r) = \mu_o nI/2\ \pi r, \tag{1}$$

where n is the number of turns each carrying a current I, and r is the distance from the major torus axis. Here the magnetic induction is in tesla, I in amps, r in meters and $\mu_o = 4\pi \times 10^{-7}$ H/m. The magnetic field varies in the ideal case as 1/r. The force per unit·length exerted on the conductor is

$$f_\rho = \mu_o n\ I^2/4\pi r. \tag{2}$$

The conductor is subjected to pure tension if f_ρ acting on a conductor element with radius of curvature ρ is balanced by the tensile force T. This leads to

$$\rho = T/f_\rho\ . \tag{3}$$

The solution of eq. (3) leads to the so-called "ideal D" contour for the conductor [1] as shown in Fig. 1.

Unlike that of circular coils, the radius of curvature ρ for the ideal D coil varies with r as

$$\rho = k \cdot r, \tag{4}$$

with

$$k = \frac{1}{2}\ \ell n\ r_2/r_1. \tag{5}$$

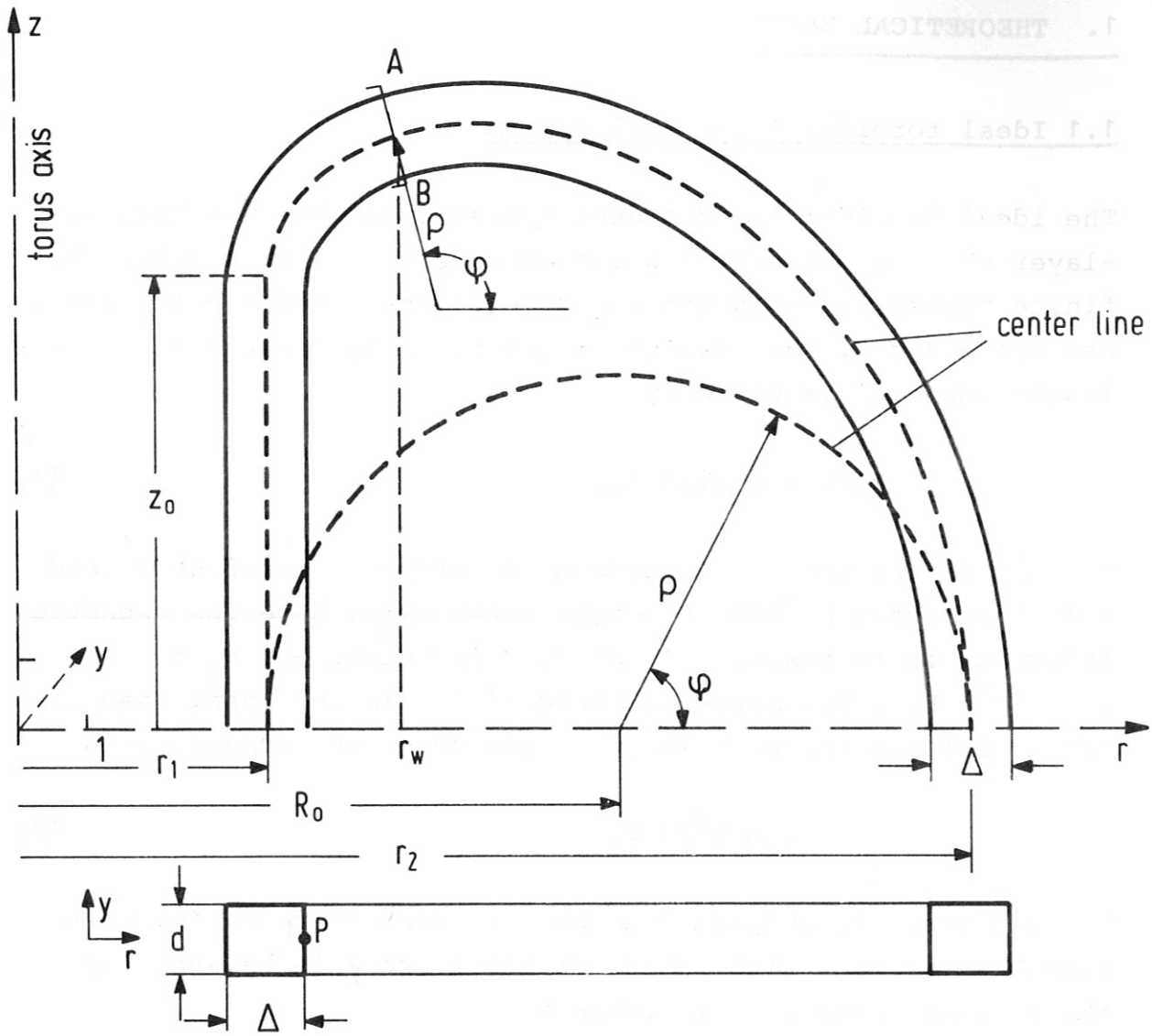

Fig. 1 Scheme of a circular and a D-coil.

In Fig. 1 the "ideal D" contour is shown as the center line of the D-coil. The current I flows in the center line. The "ideal D coil" is constructed by using the "ideal D" contour as center line of a coil with radial width Δ.

1.2 Sectored toroidal coil system ("real coils")

Taking into account the finite number n of the coils, we take for the magnetic induction in the coil bore ($z = 0$; $y = 0$; $r_1+\Delta/2 \leq r \leq r_2-\Delta/2$) for circular and D-coils [2,3]

$$B(r) = \frac{\mu_o n I}{2\pi r} \left[1 + \frac{1}{(r/r_1)^n - 1} + \frac{1}{(r_2/r)^n - 1}\right]. \qquad (6)$$

Comparing eq. (6) with eq. (1) shows that B(r) calculated with eq. (6) deviates as r goes to $r_1+\Delta/2$ and to $r_2-\Delta/2$, especially for small n values from the 1/r relation. The maximum value B_{max} is attained at the point P (see Fig. 1) at $r = r_1+\Delta/2$. Eq. (6) rewritten as a function of B_{max} reads

$$B(r) = \frac{B_{max}\, r_1 (1+\Delta/2r_1)}{\left[1 + \frac{1}{(1+\frac{\Delta}{2r_1})^n - 1}\right]} \frac{1}{r} \left[1 + \frac{1}{(\frac{r}{r_1})^n - 1} + \frac{1}{(\frac{r_2}{r})^n - 1}\right]. \qquad (6^1)$$

In calculating B_{max} the third term in eq. (6) was neglected because $[r_2/r_1+\Delta/2)]^n >> 1$.

As a consequence of the fact that B(r) does not vary as 1/r, "ideal D coils" are not in pure tension - they are also subjected to bending forces - operating in a sectored toroidal coil system. Modifications for eqs. (2) and (4) are necessary to obtain contours for D-coils ("real D coils") subjected to pure tension. The "real D coils" are also called "optimized" or "modified D coils".

Moses and Young [4] calculated the magnetic force per unit length for sectored toroidal coil systems as

$$f_\varphi = \frac{\mu_o n I^2}{4\pi r} \left[1 + \frac{1}{n}\left(\cos\varphi + \frac{r}{\varphi} \ln \frac{1.284r}{c \cdot n}\right)\right], \qquad (7)$$

where c is the radius of a circular coil cross-section. In this approximation, the current is assumed to flow in the center of the circular winding as a filamentary current on which the magnetic force f_φ acts. In fact, f_φ varies over the coil winding as the magnetic field varies; for this reason, the force value calculated with eq. (2) or (7) is also interpreted as a mean force per unit length.

For square coil cross-section with width w one may replace [4] c with 0.593 w(d = Δ = w, see fig. 1).

The radius of curvature ρ for "real D-coils" is given by [4]:

$$\rho = r \left[\frac{\rho_2}{r_2}\left(1 + \frac{1}{n}\right) - \frac{1}{n} \ln \frac{r}{r_2}\right] / \left(1 + \frac{1}{n} \cos\varphi\right), \qquad (8)$$

where ρ_2 is the radius of curvature at r_2. Once ρ_2/r_2 is selected, ρ can be calculated as a function of r and the angle φ. The ρ_2/r_2 value is determined by fixing the number of coils and the values of r_1 and r_2 as in shown in ref. [4].

Because f_ρ and ρ depend on r and φ simultaneously (eq. (7) and (8)) these values cannot be calculated directly in these forms. One way is to calculate the contours numerically to get a relation between r and φ. The aim of this work is, however, to get simple analytical expressions for coil design parameters, and so we do not choose this way. We shall eliminate one of the two variables (r or φ) to get f_ρ and ρ as a function of one variable and compare the results with numerically calculated fields and forces.

2. ANALYTICAL EXPRESSIONS

2.1 Circular coils

The magnetic field is calculated with eq. (6) to get the maximum field value at the windings.

For the magnetic force per unit length we use eq.(7) and eliminate $\cos\varphi$ with

$$\cos\varphi = (r + \rho - r_2)/\rho \ . \qquad (9)$$

With the definition of the aspect ratio A_m

$$A_m = \frac{R_o}{\rho} \qquad (10)$$

the force per unit length is given by

$$f_\varrho = \frac{\mu_o n I^2}{4\pi r} \left\{1 + \frac{1}{n \cdot \varrho} \left[(r - \varrho A_m) + r \ln \frac{2.24 r}{w \cdot n}\right]\right\} . \qquad (11)$$

The centripetal force F_C per coil is calculated from

$$F_C = \int_{\text{contour}} f_{\varrho,r}\, ds, \qquad (12)$$

where $f_{\varrho,r}$ is the force component per unit length directed in the r-direction (see Fig. 1) and ds is the element of the coil contour. For circular coils F_C is given by

$$F_C = 2\varrho \int_0^\pi f_\varrho \cos\varphi \, d\varphi . \qquad (13)$$

In the "ideal case" with

$$f_\varrho = \mu_o n I^2 / 4\pi r \qquad (2)$$

the integration gives

$$F_C = \frac{\mu_o n I^2}{2} \left\{\frac{\sqrt{A_m^2 - 1} - A_m}{\sqrt{A_m^2 - 1}}\right\} . \qquad (14)$$

If the current I is eliminated by eq. (1), the centripetal force can be expressed as a function of the maximum magnetic induction $B_{max} = B(r_1)$:

$$F_C = \frac{2\pi^2}{\mu_o n} B_{max}^2 R_o^2 \left[(A_m - 1)/A_m\right]^2 \left\{\frac{\sqrt{A_m^2 - 1} - A_m}{\sqrt{A_m^2 - 1}}\right\} \qquad (15)$$

The centripetal force increases quadratically with the major torus radius R_o and with the maximum magnetic field for constant A_m. The dependence on the aspect ratio A_m is shown in Fig. 2.

The centripetal force shows a strong dependence on the aspect ratio A_m with a maximum value at $A_m = 1.75$. The appearance of the maximum is a consequence of the fact that with const. B_{max} and R_o the current I and the radius changes with varying A_m;

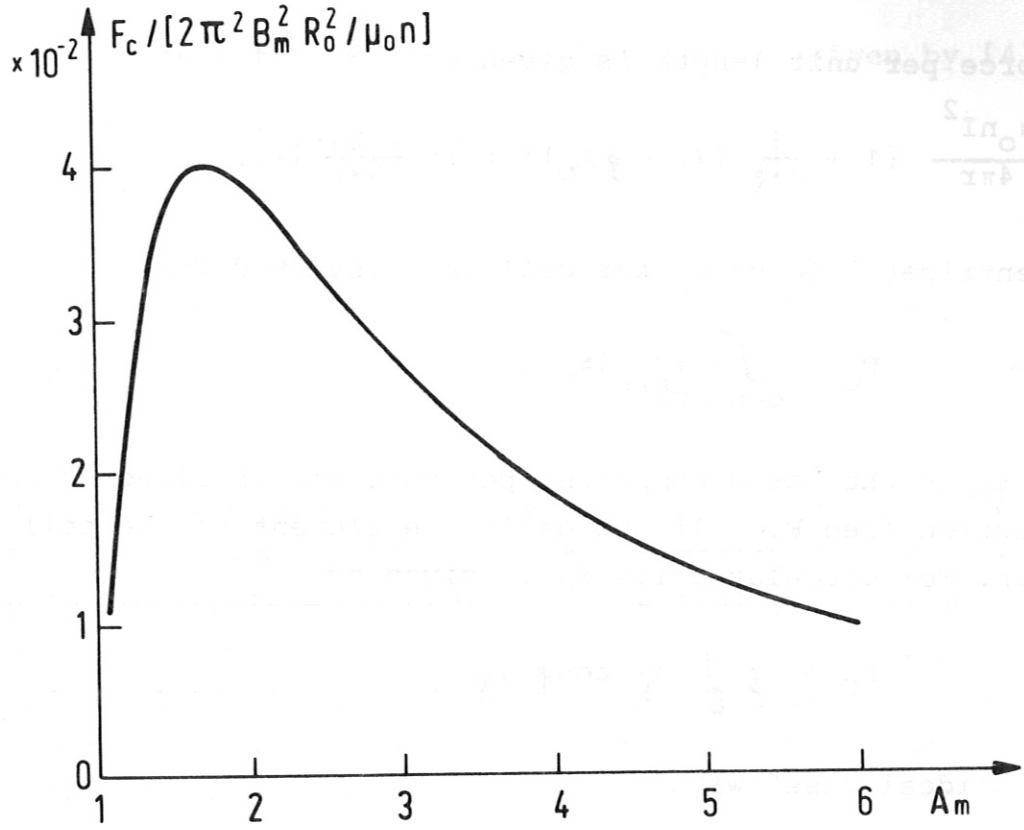

Fig. 2 Dependence of the centripetal force on the aspect ratio for circular coils according to eq. (15) for the "ideal case".

with increasing A_m the current I increases whereas the radius ϱ decreases. The negative sign for F_C describes the fact that F_C is directed towards the torus center.

For the sectored case ("real case") with circular coils using eq. (11) the centripetal force is then

$$F_C = \frac{\mu_o n I^2}{2} \frac{\sqrt{A_m^2-1} - A_m}{\sqrt{A_m^2-1}} \left\{1 - \frac{A_m}{n} + \frac{1}{2n}\left[\frac{1}{\sqrt{A_m^2-1} - A_m} - \sqrt{A_m^2-1} + A_m\right]\right\}, \quad (16)$$

where the condition (for d = w, see Fig. 1)

$$n \cdot w \leq 2\pi \; R_o \; (1 - A_m^{-1}) \quad (17)$$

must be fulfilled with allowance for the fact that the number n of coils with square coil cross-section w x w is limited by the circumference of the coil system at the inner side r_1 (see Fig. 1).

Eq. (16) can be rewritten as

$$F_C = F_C \text{ (ideal)} \cdot C, \tag{18}$$

with

$$C = \left\{1 - \frac{A_m}{n} + \frac{1}{2n}\left[\frac{1}{\sqrt{A_m^2-1} - A_m} - \sqrt{A_m^2-1} + A_m\right]\right\} \tag{19}$$

as the correction factor for the sectored toroidal magnet system. For an increasing number of coils n the correction factor approaches the value 1, and F_C is identical with F_C (ideal) given by eq. (14). The depencence of the correction factor on the aspect ratio A_m is shown in Fig. 3.

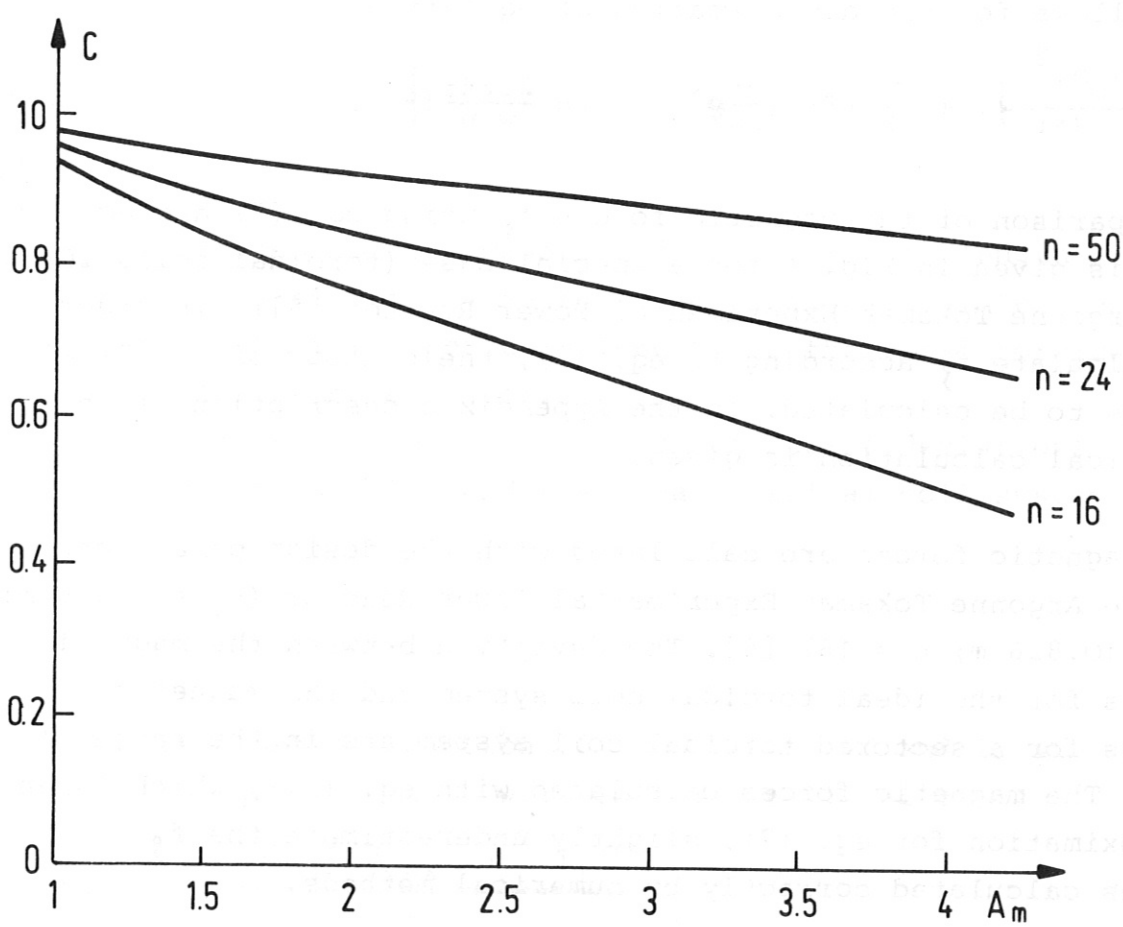

Fig. 3 Dependence of the correction factor C (eq. (19)) on the aspect ratio A_m for coil systems with n = 16, 24 and 50 coils.

2.2 D-coils

As for the circular coils we use for the magnetic field calculation eq.(1)or eq.(6).

The magnetic force per unit length f_ϱ is calculated for the "real case" from eq. (7). To eliminate the radius of curvature ϱ and $\cos\varphi$, we use the formulae derived for the "ideal case" [5], and get f_ϱ as a function of r.

With

$$\varrho = k \cdot r \tag{4}$$

and $$\cos\varphi = \frac{1}{k} \ln \left(\frac{r}{r_2} e^k\right) \tag{20}$$

it follows for the approximation of eq.(7) that

$$f_\varrho = \frac{\mu_o n I^2}{4\pi r} \left\{1 + \frac{1}{nk} \left[\ln \left(\frac{r}{r_2} e^k\right) + \ln \frac{2.24 r}{w \cdot n}\right]\right\} . \tag{21}$$

A comparison of the magnetic forces f_ϱ using eq. (7) and eq. (21) is given in Fig. 4 for a special case (toroidal coils for the Argonne Tokamak Experimental Power Reactor [6]). In order to calculate f_ϱ according to eq. (7), the contour of the "real D" has to be calculated. In the Appendix a description of the numerical calculation is given.

The magnetic forces are calculated with the design parameters of the Argonne Tokamak Experimental Power Reactor (r_1 = 2.566 m; r_2 = 10.826 m; n = 16) [6]. The deviation between the magnetic forces for the ideal toroidal coil system and the magnetic forces for a sectored toroidal coil system are in the range of 10 %. The magnetic forces calculated with eq. (21), which is an approximation for eq. (7), slightly underestimate the f_ϱ values calculated correctly by numerical methods.

The centripetal force for the "ideal D" contour is given by the product of $f_\varrho(r_1)$ times the straight section 2 z_o [5] of the D-coil (integral (13) is zero for this case) and reads as

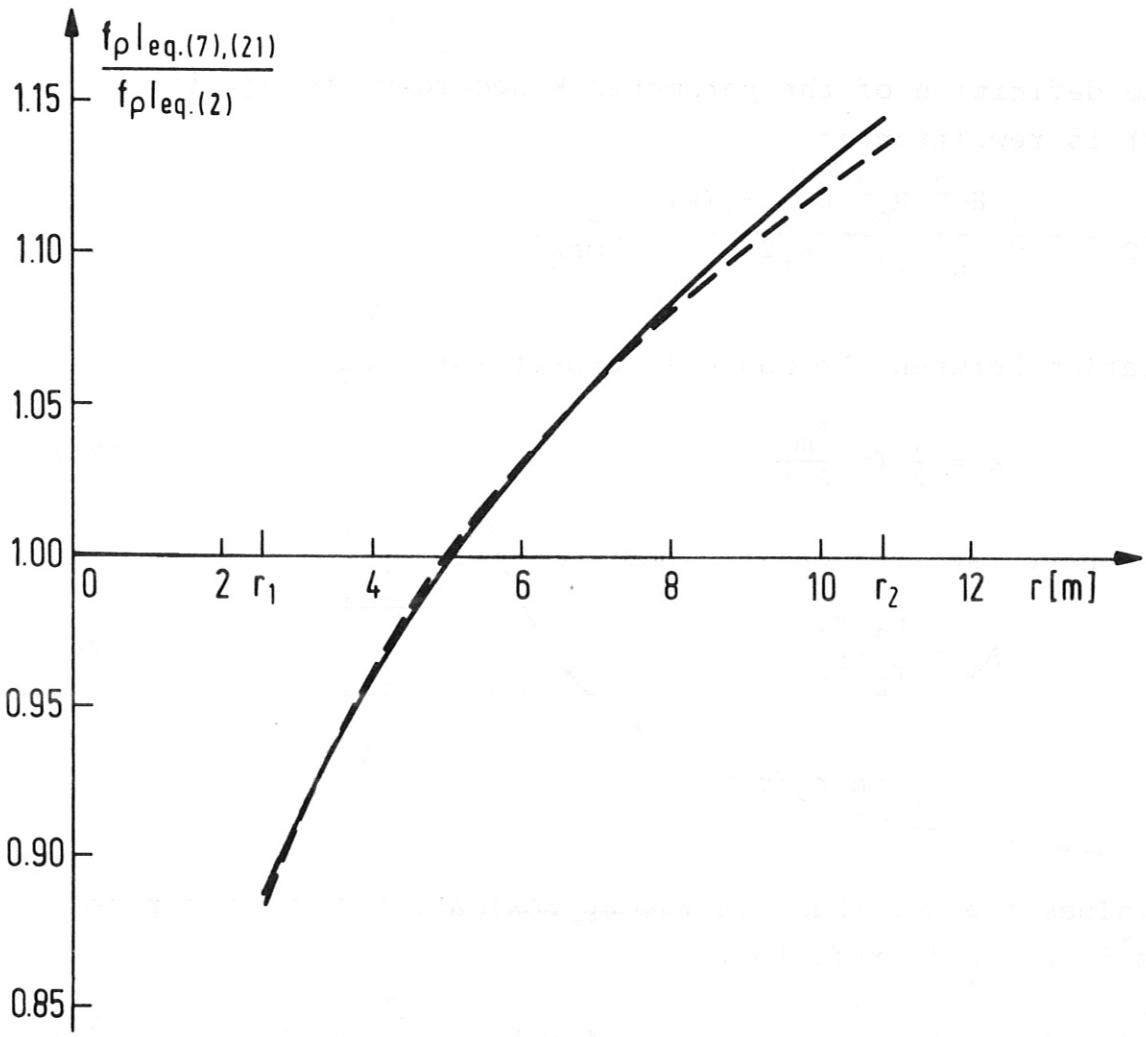

Fig. 4 Deviations of the magnetic forces per unit length calculated for the sectored toroidal coil system (eq. 7) from the force per unit length for the ideal toroidal coil system (eq. (2)).
The dashed line shows the corresponding deviations between eq. (21) and the ideal toroidal coil system (eq. (2)).

$$F_C = -\frac{1}{2}\,\mu_o n I^2\, k e^k\, I_1(k) \qquad (22)$$

(I_1 = modified Bessel function of the first kind and first order). With eq. (1), F_C is written for the "ideal D" as

$$F_C = -\frac{1}{n}\,\frac{2\pi^2 r_1^2\, B_{max}^2\, k\, e^k\, I_1(k)}{\mu_o}\,. \qquad (23)$$

To compare the centripetal forces of "ideal D" coils and ideal circular coils, r_1 is expressed by $R_o = (r_2 + r_1)/2$.

With the definition of the parameter k according to eq. (5) eq. (23) is rewritten as

$$F_C = -\frac{1}{n}\,\frac{8\pi^2\, R_o^{\,2}\, k e^k\, I_1(k)}{\mu_o\,(1+e^{2k})^2}\; B_{max}^2 . \tag{24}$$

The relation between the magnetic aspect ratio A_m and k is

$$k = \frac{1}{2}\,\ell n\,\frac{A_m+1}{A_m-1}\,, \tag{25}$$

where we have used the definitions

$$A_m = \frac{r_2+r_1}{r_2-r_1} \tag{26}$$

and

$$k = \frac{1}{2}\,\ell n\, r_2/r_1 . \tag{5}$$

For k values smaller than 0.4 the approximation $A_m \approx 1/k$ can be used as is shown in ref. [5].

The ratio of the centripetal force for "ideal D coil" (eq. (24)) and that for a circular coil (eq. (15); ideal case) is given by

$$\frac{F_{C,D}}{F_{C,O}} = -\frac{1}{2}\,\frac{\ell n\,[(A_m+1)/(A_m-1)]\cdot(A_m+1)\cdot I_1(k(A_m))}{[\sqrt{A_m^2-1}\;-A_m]}, \tag{27}$$

where we have used eq. (25) eliminating the parameter k, and where n, R_o and B_m are constants. The curve corresponding to eq. (27) is shown in Fig. 5.

For "real D-coils" the centripetal force can be calculated in the same manner as for the "ideal D" because integral (13) is also zero; the integration is carried out for this case above the "real D" contour, which can be calculated as shown in the Appendix.

F_C is calculated as

$$F_C = -f_\varphi\;(\varphi=\pi)\cdot 2z_o . \tag{28}$$

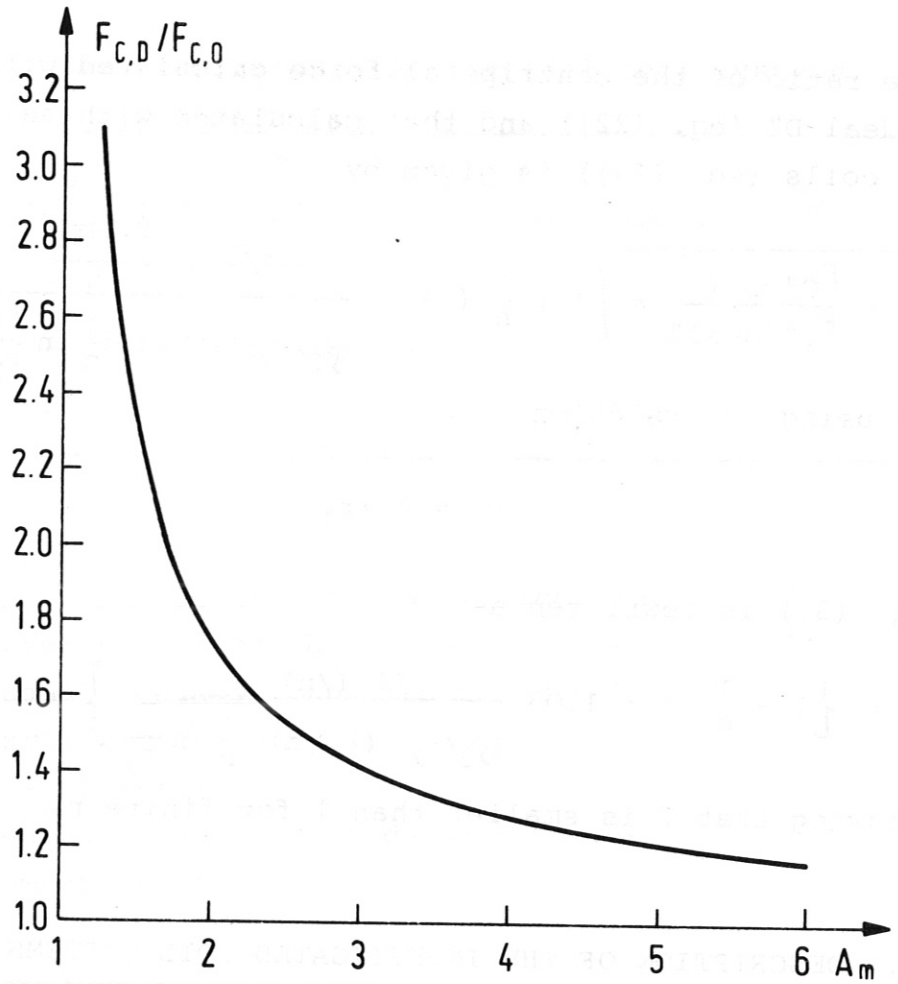

Fig. 5 Ratio of the centripetal force for D-coils and circular coils versus the aspect ratio A_m corresponding to eq. (27).

With eqs. (7) and (8) F_C is given for "real D" coils by

$$F_C = -\frac{\mu_o n I^2}{2}\left\{1+\frac{1}{n}\left[-1+\frac{(1-1/n)\cdot \ell n\,\frac{2.24 r_1}{w\cdot n}}{(\varrho_2/r_2)\cdot(1+1/n)-\frac{1}{n}\,\ell n\,\frac{r_1}{r_2}}\right]\right\}\cdot k e^k\, I_1(k). \qquad (29)$$

Using eq. (5) the current I can be eliminated by $B_{max} = B(r_1+\Delta/2)$, and F_C is given as a function of the maximum magnetic induction:

$$F_C = -\frac{2\pi^2\, r_1^2 (1+2\frac{\Delta}{r_1})^2\, B_{max}^2}{n\mu_o\left[1+\frac{1}{(1+\frac{\Delta}{2r_1})^2-1}\right]}\left\{1+\frac{1}{n}\left[-1+\frac{(1-1/n)\,\ell n\,\frac{2.24 r_1}{w\cdot n}}{(\varrho_2/r_2)\cdot(1+1/n)-\frac{1}{n}\,\ell n\,\frac{r_1}{r_2}}\right]\right\} k e^k\, I_1(k) \qquad (30)$$

Δ is the radial width of the coil winding. For coils with square cross-section one has $\Delta = w$. For rectangular coil cross-section we use the relation $w = \sqrt{\Delta \cdot d}$ (see Fig. 1).

The ratio of the centripetal force calculated with eq. (2) for "ideal D" (eq. (22)) and that calculated with eq. (7) for "real D" coils (eq. (29)) is given by

$$\Gamma = \frac{F_{C"real"}}{F_{C"ideal"}} = \left\{1 + \frac{1}{n}\left(-1 + \frac{(1-1/n)\ \ell n\ \frac{2.24 r_1}{w \cdot n}}{(\varrho_2/r_2)(1+1/n) - \frac{1}{n}\ \ell n\ \frac{r_1}{r_2}}\right)\right\} \tag{31}$$

By using the relation

$$n \cdot w = 2\pi \cdot r_1 \tag{32}$$

eq. (31) is rewritten as

$$\Gamma = \left\{1 - \frac{1}{n}\left(1 + 1.03\ \frac{(1-1/n)}{(\varrho_2/r_2)\ (1+1/n) - \frac{1}{n}\ \ell n\ \frac{r_1}{r_2}}\right)\right\}, \tag{33}$$

showing that Γ is smaller than 1 for finite n.

3. DESCRIPTION OF THE INVESTIGATED COIL SYSTEMS

To compare coil parameters derviced from analytical formulas eqs. (1, 2, 6, 11, 14, 15, 16, 21, 22, 29) described in the last two sections, three toroidal coil systems are designed for which the corresponding parameters were calculated numerically by computer programs. The toroidal coil systems consist of a small circular coil system (TI), a large circular coil system (TII) and a large D-coil system (TIII) with "ideal D-coils".

The data are listed in Table 1.

In Fig. 1 the center lines of the D-coil and the circular coil are identical with the center lines of TIII and TII if one uses the scale of 1 cm corresponding to 1 m

The numerical calculations were made with the HEDO computer program [7]. In these calculations the current distribution is idealized in such a way that the total current I is subdivided

Table 1 Data for the superconducting toroidal coil systems.

System:	R_o [m]	r_1 [m]	r_2 [m]	Δ [m]	d [m]	$\langle j \rangle$ [A/cm^2]	A_m	n
TI (circular)	2.07	1.55	2.59	0.1	0.1	10^4	3.94	40
TII (circular)	9.135	3.5	14.77	0.72	0.54	1.5×10^3	1.62	24
TIII (D-coil)	9.135	3.5	14.77	0.72	0.54	1.5×10^3	1.62	24

R_o : Major torus radius
r_1 : Inner radius of the center line (see Fig. 1)
r_2 : Outer radius of the center line (see Fig. 1)
Δ : Radial width of the winding (see Fig. 1)
d : Axial width of the winding
A_m : $2\,R_o/[r_2-r_1]$
$\langle j \rangle$: Mean average current density: $I/\Delta \cdot d$
n : Number of coils

into q "filamentary currents" i = I/q, where the current i flows in the center of a cross-sectional coil element with an area $(\Delta \cdot d)/q$. The number q is given by the subdivision of the winding cross section $q = n_r \cdot n_y$, where n_r is the number of subdivision in the r-direction, and n_y the number of subdivisions in the y-direction.

For TI we use q = 5x5, for TII and TIII q = 8x6. For the subdivision into p segments in the circumferential direction we use: p = 25 for TI and p = 31 for TII and TIII. The program calculates the magnetic forces per unit length for the center of each coil volume element. The centripetal force for a coil is obtained by summing up the radial forces $f_{s,r}$ of all coil elements.

For the stress calculations we use the finite element program SOLID SAP IV [8]. As element a 20-node isoparametric hexadron is used. The method of the stress calculation is described in detail in ref. [9].

4. COMPARISON OF ANALYTICAL AND NUMERICAL RESULTS

4.1 Magnetic Fields

We compare the magnetic field values on the central line (y=0, z=0, see Fig. 1) calculated with eq. (1), eq. (6) and the HEDO computer program. In designing superconducting magnet systems the maximum magnetic induction B_{max} in the coil winding is an important parameter. In our nomenclature B_{max} appears at the point P with the coordinates $r = r_1 + \Delta/2$, $y = 0$, $z = 0$.

In Fig. 6 the magnetic field in the coil bore is shown for the TIII coil system (see Table 1). The agreement between the numerically computed values and the values according to eq. (6) is very close. Greater deviatins only occur at $(r_2 - \Delta/2)$, where the numerical value is 4.65 T, whereas the analytically calculated value is 4.25 T. For the TII system the accuracy is the same as for TIII.

In Table 2 some results including also TI (small circular coil system) are listed.

Table 2 Comparison of maximum magnetic field values

System	B_{max} (numerical) in tesla	B_{max} (eq.(1), $r=r_1+\Delta/2$) tesla	B_{max} (eq.(6), $r=r_1+\Delta/2$) tesla	$B(R_o)$ (numerical) tesla	B_{max} (eq.(1), $r=r_1$) tesla
T I	6.8	5.15	7.10	3.95	5.3
TII, TIII	7.9	7.25	8.0	3.0	8.0

The differences between the numerical results and the results from eq. (1) are large especially for the TI coil system.

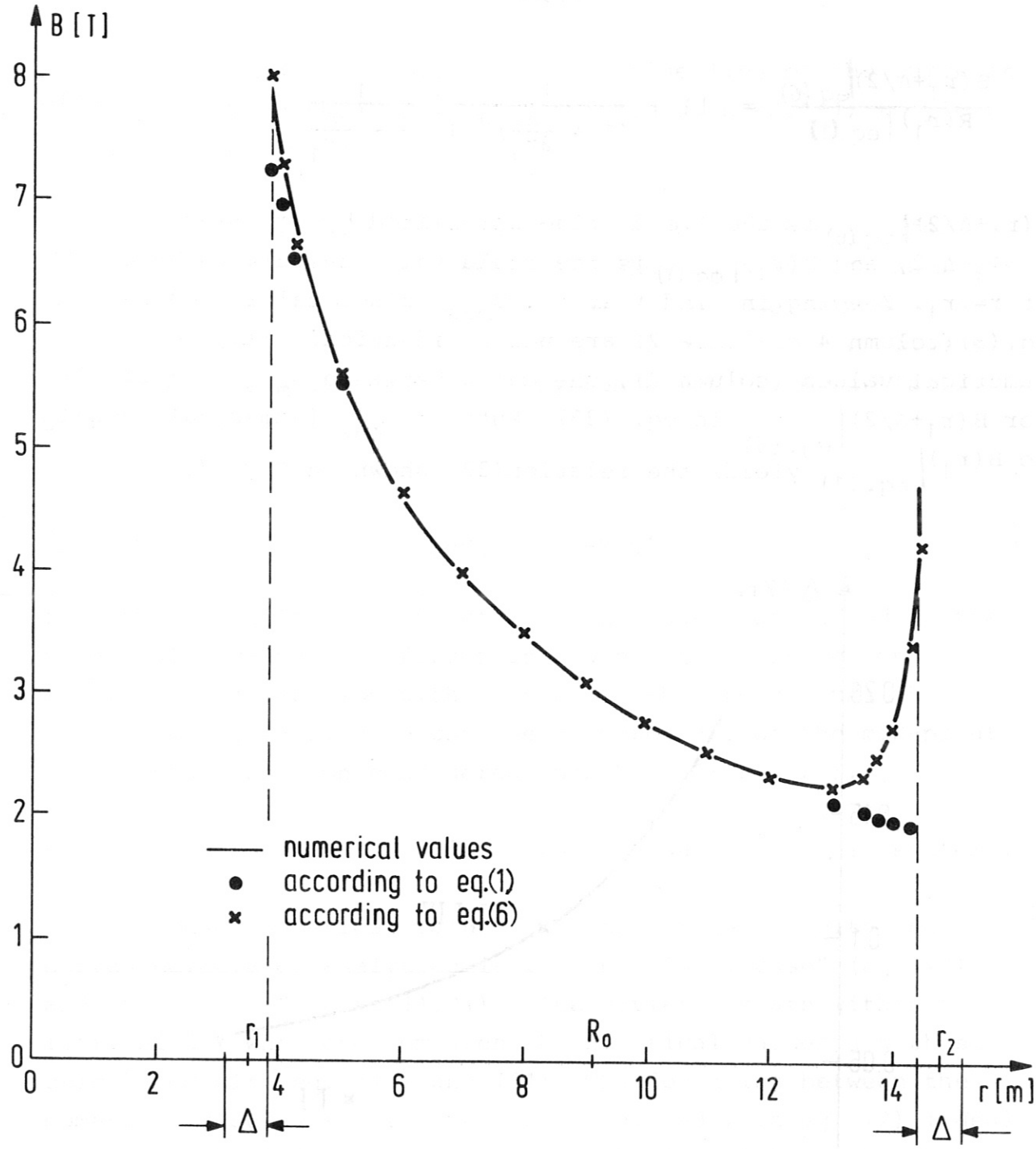

Fig. 6 Magnetic field versus distance from the major torus axis in the coil bore for the system T III (see Table 1).

Eq. (1) (ideal case) gives the correct result only for the special case if the following relation between $\Delta/2r_1$ and n

$$(1 + \frac{\Delta}{2r_1})^{n} - (1 + \frac{\Delta}{2r_1})^{n-1} = 1 \qquad (32)$$

is fulfilled. This formula was derived by introducing the ratio

$$\frac{B(r_1+\Delta/2)\big|_{eq.(6)}}{R(r_1)\big|_{eq.(1)}} = \left[1 + \frac{1}{(1+\frac{\Delta}{2r_1})^n - 1}\right] \frac{1}{1+\frac{\Delta}{2r_1}} \quad . \tag{33}$$

$B(r_1+\Delta/2)\big|_{eq.(6)}$ is the field value calculated by eq.(6) at $r = r_i+\Delta/2$, and $B(r_1)\big|_{eq.(1)}$ is the field value calculated by eq.(1) at $r = r_1$. Keeping in mind that the B_{max} values calculated by eq.(6) (column 4 of Table 2) are nearly identical with the numerical values (column 2), one can substitute B_{max} (numerical) for $B(r_1+\Delta/2)\big|_{eq.(6)}$ in eq. (33). Putting B_{max} (numerical) equal to $B(r_1)\big|_{eq.(1)}$ yields the relation (32) shown in Fig. 7.

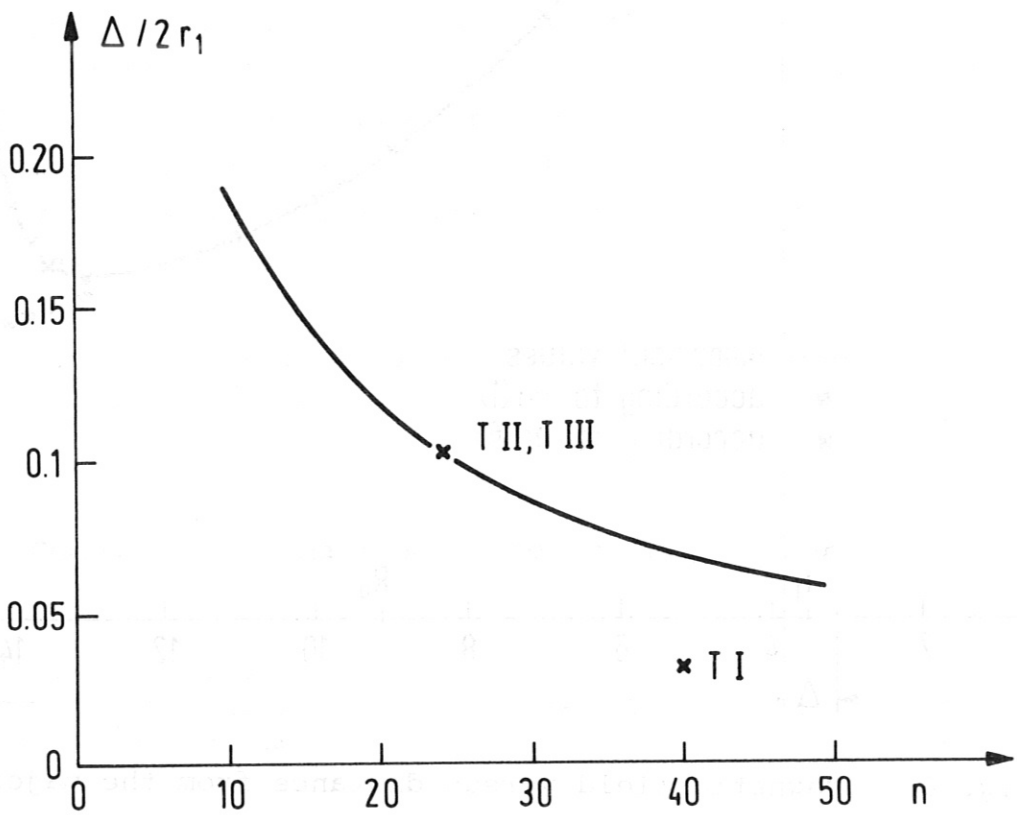

Fig. 7 Dependence of the ratio coil thickness Δ to r_1 on the coil number according to eq. (32).

x : corresponding values for the T I, T II and T III toroidal coil systems (Table 1)

For coil systems for which the $\Delta/2r_1$ value lies on the curve in Fig. 7, the B_{max} value can be calculated with eq. (1) to yield the same accuracy as with eq. (6).

In Fig. 7, $\Delta/2r_1$ values over the coil number n are given for the three coil systems investigated, showing that for the T I system eq. (32) is not satisfied. The difference between the numerical value and that calculated with eq. (1) (see columns 2 and 6 of Table 2) for the T I system demonstrate the facts shown in Fig. 7.

4.2 Mean magnetic forces per unit length

The comparison is carried out in such a way that we add up the numerically calculated forces in a winding cross-section inclined at an angle φ with respect to the r-axis. As the corresponding r-value we use the r-coordinate of the mid-point of the cross-section considered (see Fig. 1; $r = r_w$).

Results are shown in Fig. 8 for the T I and T III coil systems.

In both cases numerical values are shown together with the curves calculated analytically for the "ideal case" (eq. (2)) and "real case " (eqs.(11,21)). The deviations are within a limit of 5 % when one compares the numerical values and those calculated with eq. (11) and (21). The deviation between the numerical results and the values calculated with eq. (2) (ideal case) for the T I design approaching r_2 are about 10 %. The values for the large circular coil system are not shown because they are similar to the results of Fig. 8.

4.3 Centripetal forces per coil

The centripetal forces are calculated for circular coils with eq. (14) and eq. (16), and for D-coils we use eq. (22) and eq. (29).

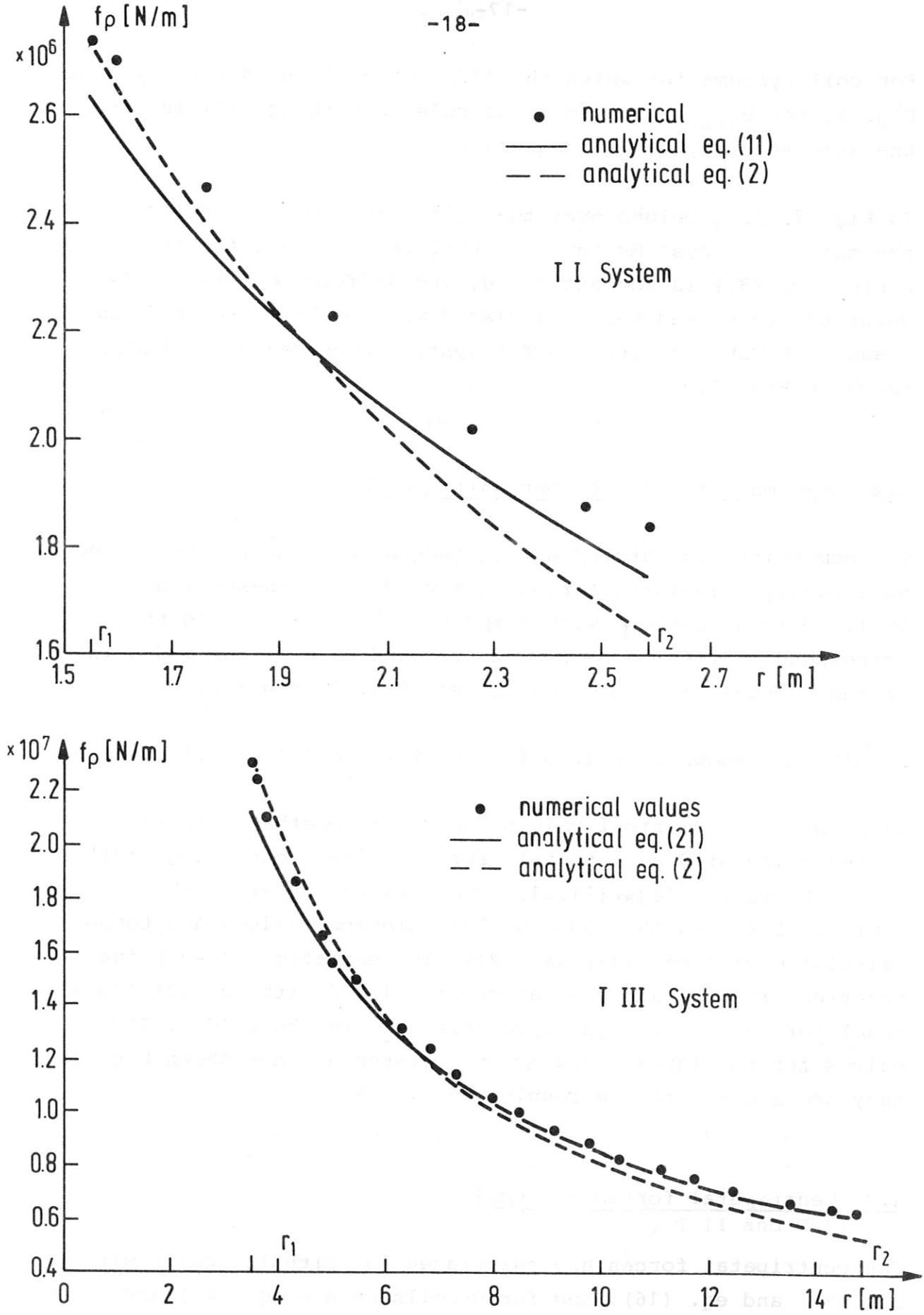

Fig. 8 Mean radial magnetic force per unit length versus distance from the major torus axis for the T I and T III coil systems

In Table 3 the centripetal forces are collected.

Table 3 Centripetal forces for the three coil systems T I, T II and T III calculated analytically and numerically

System	F_c [N] eq.(14)	F_c [N] eq.(16)	F_c [N] eq.(22)	F_c [N] eq.(29)	F_c [N] numerically
T I	-8.50×10^5	-6.85×10^5			-7.0×10^5
T II	-1.48×10^8	-1.30×10^8			-1.17×10^8
T III			-2.90×10^8	-2.50×10^8	-2.63×10^8

From Table 3 it is seen that the F_c values calculated with eqs. (16) and (29) with allowance for the fact that the toroidal coil system is sectored show better agreement with the numerically calculated F_c values than those calculated with eqs. (14) and (22) (ideal case).

The centripetal force calculated with eqs. (14) and (22) are much larger than the numerically calculated ones. The fact that F_c calculated with eq. (14) gives the largest value can be seen from Fig. 8 for the T I system because the differences between f_ς at $r = r_2$ and $r = r_1$ are largest and therefore integral (13) gives the largest value.

For a "real D" coil with the same z_o, n and I values ($2z_o$ = straight part of coil) the centripetal force is reduced to -2.5×10^8 N per coil (eq. (29), 5th column of Table 3). The ratio between the numerically calculated centripetal forces T III and T II is 2.24; the corresponding value according to eq. (27) is 2.15 (see Fig. 5).

4.4 Stresses

The stresses for the T I system are calculated by the finite element method [9]. The winding of the superconducting test coil consists of a NbTi conductor with a copper-to-superconductor ratio of 2.5:1. For the elastic modules E a value of 10^7 N/cm^2 was assumed [10] with allowance for the conductor composition (a more detailed description is given elsewhere [11]).

In this section, we investigate if the force loading of the coil using the values from the HEDO computer program [7] or the analytical values from formula (11) derived in section two give different stress values for the coil winding.

The variation of the radial force density calculated numerically with HEDO is shown in Fig. 9 together with force density f_o calculated with eq. (11). ($f_o = f_g/\Delta \cdot d$; $\Delta \cdot d$ is the winding cross-section).

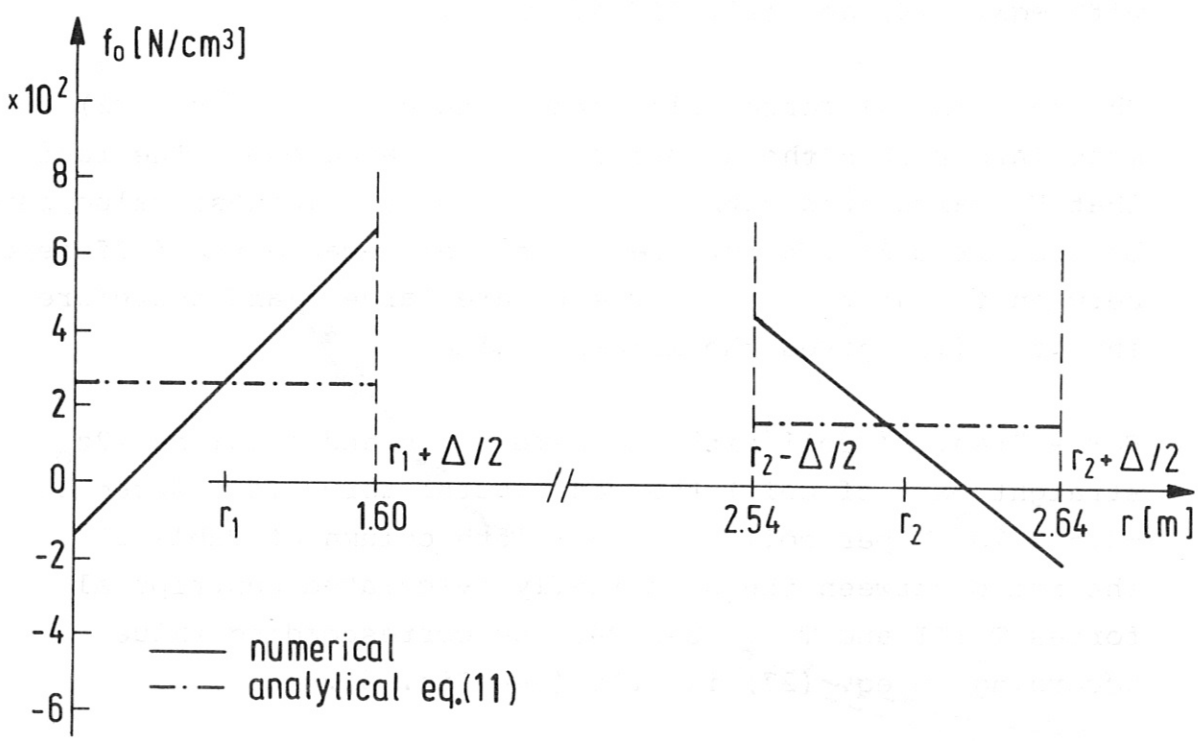

Fig. 9 Variation of the magnetic force density across the coil winding at the inner and outer parts of the T I coil (z = 0; y = 0)

The finite element program calculates σ_{xx}, σ_{yy}, σ_{zz}, σ_{xy}, σ_{yz} and σ_{zx}, from which the effective (or reference) stress σ_{eff} [12]

$$\sigma_{eff}=\left\{\sigma_{xx}^2+\sigma_{yy}^2+\sigma_{zz}^2-\sigma_{xx}\sigma_{yy}-\sigma_{yy}\sigma_{zz}-\sigma_{zz}\sigma_{xx}+3\,(\sigma_{yx}^2+\sigma_{yz}^2+\sigma_{zx}^2)\right\}^{1/2} \qquad (34)$$

containing the normal stresses σ_{xx}, σ_{yy}, σ_{zz} and the shear stresses σ_{xy}, σ_{yz}, σ_{zx} is constructed. According to the von Mises criterion yielding of the material within an element begines when the effective stress value σ_{eff} equals the yield point stress.

The σ_{eff} values for the windings placed at the inner coil edge are shown in Fig. 10 for both cases. The σ_{eff} values calculated form the numerical force densities are only a small amount larger than those calculated from eq. (11). The good agreement between the σ_{eff} values calculated by two different force loading processes is primarily a consequence of the material properties of the coils and of the fact that the material constants are assumed to be uniform and isotropic within the winding.

5. CONCLUSIONS

The main results of this investigation are:

a) Good agreement between the numerically and analytically calculated maximum magnetic field values using eq. (6). The dependence of B(r) on the distance r from the major torus axis given by eqs.(6,6[1]) is also in good agreement with the numerically calculated values (see Fig. 6).

b) The mean magnetic forces per unit length and the centripetal forces are approximated by the analytical formulas (2, 11, 21 for magnetic forces per unit length) and formulas (14, 16, 22, 29 for centripetal forces) in such a way that for parameter studies the analytical formulas give a sufficient accuracy.

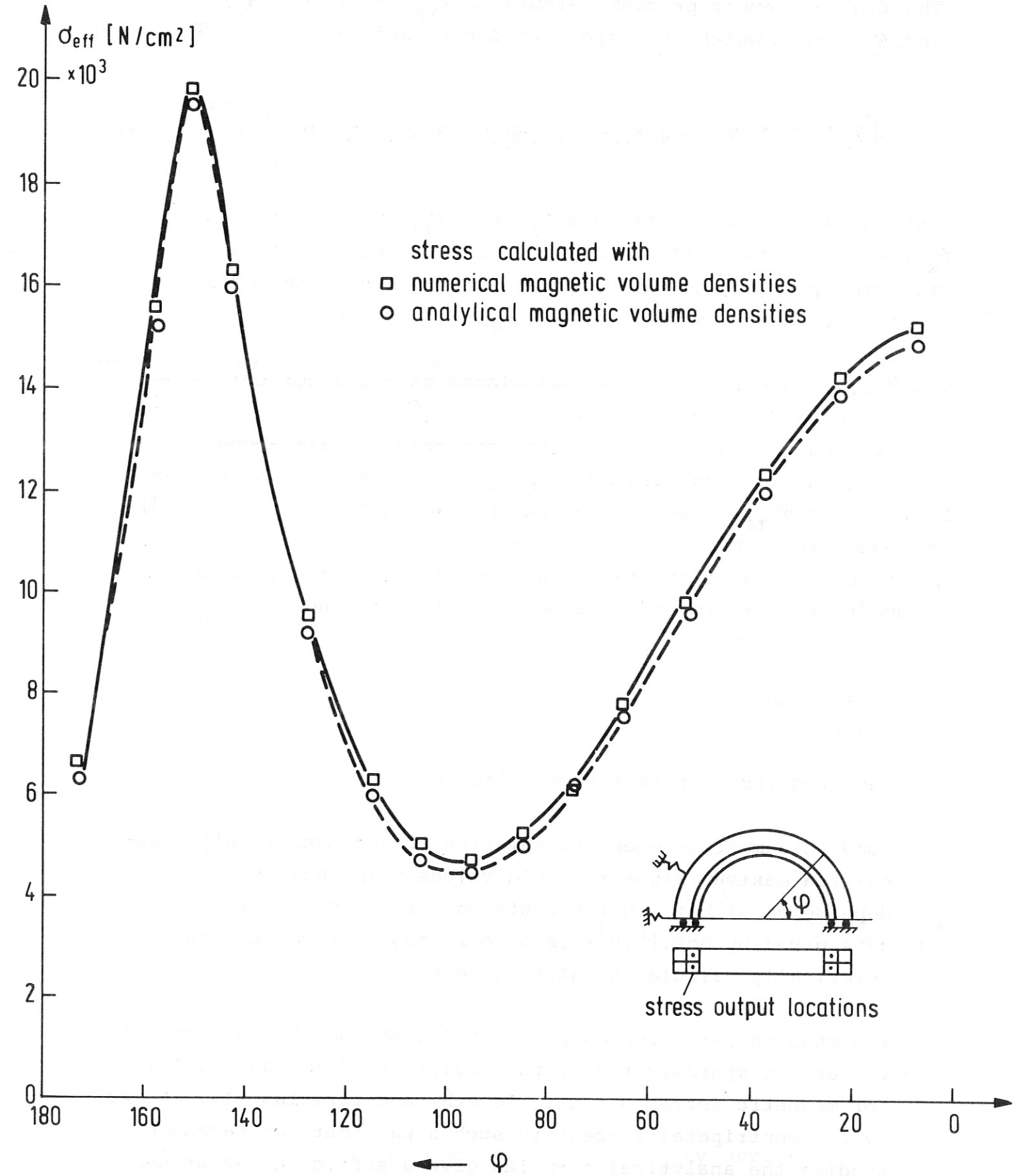

Fig. 10 Variation of the effective stress σ_{eff} for T I at the inner part of the coil (see insert) along the circumference

c) For stress calculations using the finite element method the coil loading by the magnetic body forces can be approximated by the analytical values calculated from the formulas (11) and (21).

APPENDIX

Calculation of the contour of "real D" coils("optimized"or "modified"D-coils)

"Ideal D"-coils are not in pure tension because the magnetic field does not vary as 1/r, where r is the distance from the major torus axis.

One method of getting pure tension coils is, as shown by the design team of the Tokamak Experimental Power Reactor at Argonne National Laboratory [6], to choose a $1/(\alpha_1+\alpha_2 r+\alpha_3 r^2)$ field dependence instead of a 1/r dependence. The radius of curvature ϱ is set as

$$\varrho = (\beta_1+\beta_2 r+\beta_3 r^2) = \pm \left[1+\left(\frac{dz}{dr}\right)^2\right]^{3/2} / \frac{d^2z}{dr^2}, \qquad \text{(A1)}$$

where β_1, β_2 and β_3 are constants. Eq. (A1) describes the contour of a filament in pure tension.

The coefficients β_1, β_2 and β_3 are obtained by a least squares fit to the numerical values of the field distribution calculated from the shape produced by a trial. The procedure starts with an "ideal D coil" shape for which ϱ is given as $\varrho = k \cdot r$. Then the magnetic field for the "ideal D" is calculated giving β_1, β_2 and β_3. Eq. (A1) is then solved. A new coil shape is obtained, and a new set of β coefficients are determined from the field distribution calculated from the new D-shape. This iterative process continues until a set of β coefficients generates a nearly identical set of β's.

For our investigations we used a simpler way of calculating the contour of D coils for sectored toroidal coil systems ("real D" or "optimized" D coil). Our calculation procedure is based on the results of Moses and Young [4], who showed that the contour calculated with eq. (8)

$$\varrho = r\,[\frac{\varrho_2}{r_2}\,(1+\frac{1}{n}) - \frac{1}{n}\,\ell n\,\frac{r}{r_2}]\,/(1+\frac{1}{n}\cos\varphi) \qquad (8)$$

is extremely close to the Argonne design calculated iterativly as described above [4, 13](0.8 % deviation in the maximum height). The samll differences are such as to reduce the already small bending stresses present in the Argonne design [13].

For solving the equation

$$r\,[\frac{\varrho_2}{r_2}(1+\frac{1}{n}) - \frac{1}{n}\,\ell n\,\frac{r}{r_2}]/(1+\frac{1}{n}\cos\varphi) = [1+(\frac{dz}{dr})^2]^{3/2}/d^2z/dr^2 \qquad (A2)$$

the parameter representation described in ref. [5] is used:

$$\frac{dr}{d\varphi} = -r\,[\frac{\varrho_2}{r_2}\,(1+\frac{1}{n}) - \frac{1}{n}\,\ell n\,\frac{r}{r_2}]\;\frac{\sin\varphi}{1+\frac{1}{n}\cos\varphi}\,, \qquad (A3)$$

$$\frac{dz}{d\varphi} = r[\frac{\varrho_2}{r_2}\,(1+\frac{1}{n}) - \frac{1}{n}\,\ell n\,\frac{r}{r_2}]\;\frac{\cos\varphi}{1+\frac{1}{n}\cos\varphi}\,, \qquad (A4)$$

In Fig. A1 half of the contour of a "real D" coil is shown by a computer plot using the data of the Argonne design (r_2 = 10.826 m, r_1 = 2.566 m, n = 16). The ratio $\frac{\varrho_2}{r_2}$ was calculated by the method described in [4, 13]. Fig. A1 shows the center line and the edge line of half of the coil.

ACKNOWLEDGEMENT

The author gratefully acknowledges the help of H. Gorenflo in carrying out the numerical calculations.

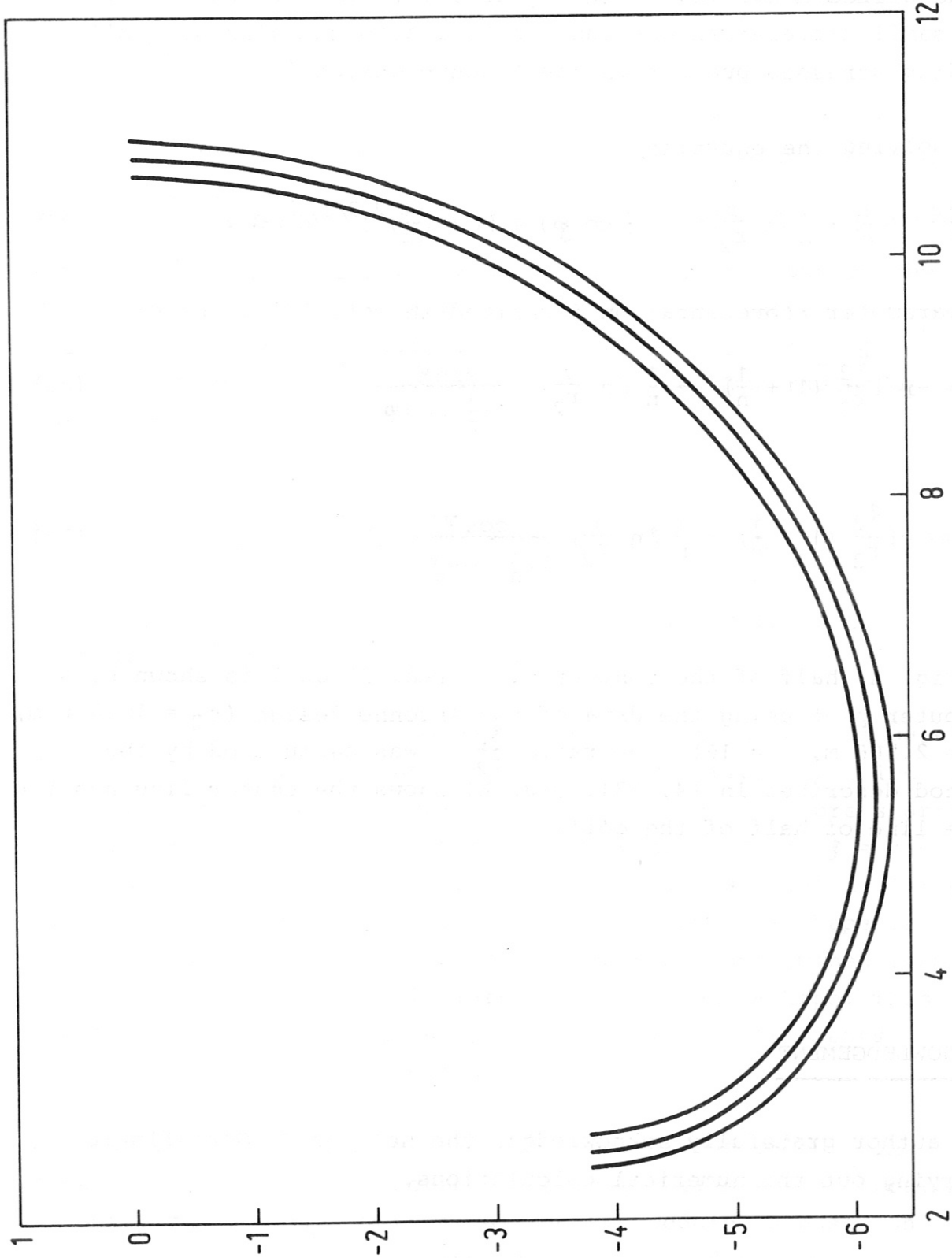

Fig. 11 Computer plot of the contour of a "real D" coil calculated from eqs. (A3) and (A4).

REFERENCES

[1] J. File, R.G. Mills, G.V. Sheffield: "Large Superconducting Magnet Designs for Fusion Reactors". MATT-848 (1971).

[2] J. Boris, A.F. Kuckes: "Closed Expression for the Magnetic Field in Two-Dimensional Multipole Configurations", MATT-473 (1966).

[3] J. File, G.V. Sheffield: "A Large Superconducting Magnet for Fusion Research", Proc. of the Fourth International Conference on Magnet Technology, p. 240 (1972).

[4] R.W. Moses, W.C. Young: "Analytic Expressions for Magnetic Forces on Sectored Toroidal Coils", Proc. Sixth Symposium on Engineering Problems of Fusion Research (San Diego 1975), p. 917 (1976).

[5] J. Raeder: "Some analytical results for toroidal magnetic field coils with elongated minor cross-section", IPP 4/141 (1976).

[6] W.M. Stacey et al.: "Tokamak Experimental Power Reactor Conceptual Design". ANL/CTR-75-2 (1975).

[7] H. Preis: "Calculation of the magnetic field, magnetic forces, and behaviour of large coil systems for fusion experiments", IPP III/24 (1976).

[8] K.J. Bathe, E.L. Wilson, F.E. Peterson: "SAP IV (A Structural Analysis Program for Static and Dynamic Response to Linear Systems)". University of California, Berkeley (1974).

[9] M. Söll, O. Jandl, H. Gorenflo: "Mechanical Stress Calculations for Toroidal Field Coils by the Finite Element Method", IPP 4/142 (1976).

[10] C.T. Sun, W.H. Gray: "Theoretical and Experimental Determination of Mechanical Properties of Superconducting Coil Composites", Proc. Sixth Symp. on Engineering Problems of Fusion Research (San Diego 1975), p. 261 (1976).

[11] M. Söll: "Simulation of Displacement and Stress Distribution of Toroidal Magnetic Field Coils", to be published.

[12] S.P. Timoshenko, J.N. Goodier: "Theory of Elasticity" 3rd ed. (Mc Graw-Hill Book Company, New York, 1970) p. 244-249.

[13] R.W. Boom, R.W. Moses, Jr., W.C. Young: "Magnet Design of Toroidal Field Coils for the UWMKA-Tokamak Systems", Nuclear Eng. and Design (to be published).

Erratum:

In Fig. 11 the radial widths (distances from the center line) of the coil winding are a factor of 2 too small.